proximity. Farm women need to be given greater access to various farm tools and equipment to carry out their work more efficiently and with minimal drudgery. Moreover, they have little access to informal education and training. It is a known fact that agricultural extension services are mainly composed of male subject matter specialists who tend to channelize knowledge and training on improved technology mainly to male farmers/workers only. The infrastructural facilities related to accommodation, transport and technical training of women workers are poor in the country. The central/state government departments, research and development institutions and non-government organizations (NGOs) should come forward to promote improved technology to enhance labour productivity and reduce drudgery of women workers. They should also recruit women extension staff for effective transfer of technologies to farm women. The ICAR-CIAE is providing necessary training on various tools and equipment to women facilitators from different states. These facilitators can act as resource persons for their own state to propagate the technologies[8].

It is estimated that participation of women in agriculture will increase to 45% by 2020 (estimated population of about 110 million) mainly because male workers get involved in other non-farm activities or migrate to towns and cities for other jobs. Therefore, women will play a major role in agriculture in future. To empower them, the following steps need to be taken: (1) Design tools/equipment keeping in view the anthropometric data of women workers. (2) Organize demonstrations and trainings for rural women on various modern tools/equipment for proper and safe operation. (3) Encourage manufacturers/entrepreneurs to fabricate improved tools and equipment and make them available in rural areas for purchase by users. (4) Assist farm women to obtain loans from banks/other organizations to procure various tools/equipment. (5) Link with central/state departments, NGOs, banks and other stakeholders to promote these improved tools and equipment.

1. Anon., Census of India 2001, Office of Registrar General and Census Commissioner, Govt of India, New Delhi, 2004.
2. Anon., Census of India 2011, Office of Registrar General and Census Commissioner, Govt of India, New Delhi, 2013.
3. Mehta, C. R., Chandel, N. S. and Senthilkumar, T., Status, challenges and strategies for farm mechanization in India. *Agricultural Mechanisation in Asia, Africa and Latin America (AMA)*, 2014, **45**(4), 43–50.
4. Gite, L. P., Majumder, J., Mehta C. R. and Khadatkar, A., Anthropometric and strength data of Indian agricultural workers for farm equipment design. Book No. CIAE/2009/4, ICAR-Central Institute of Agricultural Engineering, Bhopal, 2009.
5. Singh, S. P., Gite, L. P., Majumder, J. and Agarwal, N., Aerobic capacity of Indian farm women using sub-maximal exercise technique on tread mill. *Agric. Eng. Int.: CIGR J.*, 2008, Manuscript MES 08 001, vol. X.
6. Maiti, R. and Ray, G. G., Manual lifting load limit equation for adult Indian women workers based on physiological criteria. *Ergonomics*, 2004, **47**(1), 59–74.
7. Gite, L. P., Final Report of the Emeritus Scientist Project on Development of ergonomical design guidelines for agricultural tools, equipment and work places, ICAR-Central Institute of Agricultural Engineering, Bhopal, 2017.
8. Gite, L. P., Women in Indian agriculture. In *Ergonomics in Developing Regions: Needs and Applications* (ed. Scott, P. A.), CRC Press, 2009, pp. 291–306.

# Last 42 ky sediment chemistry of oxygen deficient coastal region of the Bay of Bengal: implications for terrigenous input and monsoon variability

T. Sarathchandraprasad[1,2,*] and
V. K. Banakar[1,3]

[1]CSIR-National Institute of Oceanography, Dona Paula, Goa 403 004, India
[2]Department of Marine Sciences, Goa University, Taleigao Plateau, Goa 403 206, India
[3]Zeib Castle, La-Oceana 2, Behind ICG, Dona Paula, Goa 403 004, India

**The discharge of terrigenous clastics by seasonal peninsular rivers is known to reach the upper slope of the eastern margin of India, which is presently impinged by the monsoon-sensitive intense oxygen minimum zone (OMZ); however, their mutual behaviour in response to changes in the intensity of past Indian summer monsoons (ISM) is not clear. The $\delta^{18}O_{G.sacculifer}$ time-series of a sediment core from the upper slope off Chennai exhibits distinct enrichment (~0.4‰) during the last glacial period (30–18 kiloyears BP: ka), and depletion (~−2.2‰) during the Holocene, suggesting a significant shift in ISM intensity. The monotonously increased terrigenous elements (Al, Ti and Mg) content and depleted $\delta^{18}O_{G.sacculifer}$ during the Holocene suggest tight-coupling between ISM and terrigenous sediment input. Highly depleted redox-sensitive Mn (<0.04%) (lesser than the source sediment content of 0.07%) throughout the last 42 kyr suggests well-sustained intense OMZ irrespective of ISM variation.**

**Keywords:** Bay of Bengal sediment, geochemistry, Holocene-LGM, OMZ, monsoon.

*For correspondence. (e-mail: sarathchandraprasad@gmail.com)

THE Indian southeastern margin sediments are dominated by terrigenous clastics derived from charnokites and granites[1], which are discharged by seasonal peninsular rivers[2]. Hence, changes in terrigenous input to the western Bay of Bengal (BoB) should reflect changes in the strength of Indian Summer Monsoon (ISM) intensity. The chemical properties of these sediments have demonstrated a significant role of climate in regulating peninsular erosion[3,4]. The enhanced terrigenous matter input to BoB by these pensinsular rivers is expected to increase productivity by enriching the photic zone nutrient load, which can affect oxygen minimum zone (OMZ) intensity.

A recent study has suggested that BoB-OMZ has reached a tipping point[5]. However, the discovery of ventilated Persian Gulf Water in the core of modern BoB-OMZ[6] and the unlikely de-oxygenation of interior of the BoB even after 2100 AD (ref. 7) together argue against the suggested 'tipping point' or its further intensification. It may be useful if the natural background status of BoB-OMZ is provided for predicting its future status under global warming scenarios. Such natural background can be obtained from reconstruction of past OMZ from sediments at water-depths within the core of modern OMZ.

ISM is mostly responsible for the development and maintenance of strong OMZ in the BoB[8,9]. The bay's OMZ (Figure 1) contains a complex mixture of aged waters[10]. Hence small changes in coastal productivity as a result of changes in terrigenous matter supply may affect its status significantly and in turn OMZ. Therefore, it is necessary to understand the past variation of BoB-OMZ in the light of ISM-driven biogeochemical processes. In this study, we present the past variation in terrigenous input and OMZ by utilizing geochemical record of sediment which is swept by the core of the modern OMZ.

A 282 cm long sediment core (GC-14A) was collected on-board ORV Sindhu Sankalp Cruise No. 50 (SSK50) at 325 m water depth off Chennai, east-coast of India (13°39′58″N; 80°34′30″E) (Figure 2) within the core of present day OMZ (Figure 1). Tests of mixed species of gently crushed and ultrasonically cleaned planktonic foraminifera (equivalent to ~1 mg of carbon) from core-top and bottom sections (0.5 cm and 281.5 cm) were radiocarbon-dated at the University of Arizona AMS facility. The measured radiocarbon ages were corrected for a reservoir age of 331 years[11], and converted into calendar age using CalPal-7 calibration[12]. The $\delta^{18}O$ measurements were carried out for 65 sections on an in-house Thermo Delta-Plus continuous flow Isotope Ratio Mass-Spectrometer (IRMS) utilizing ultrasonically cleaned 250–355 μm size tests of *Globigerinoides sacculifer* (without terminal-sac) (Figure 3). The standard precision of $\delta^{18}O$ measurement is 0.1‰. The average of long-term repeat measurements ($n = 33$) of NBS-18 (calcite) reference standard yielded $\delta^{18}O$ of −23.05‰ vPDB as against the certified value of −23.2 ± 0.1‰ vPDB. Two distinctly
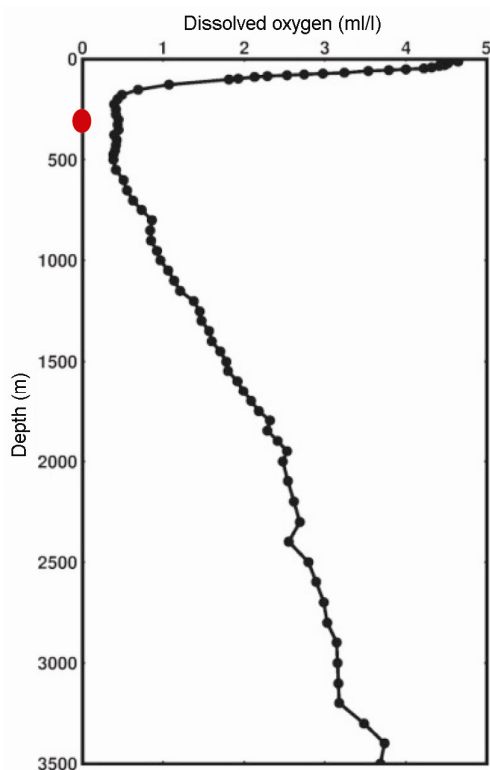


**Figure 1.** Modern vertical distribution of dissolved oxygen in the 1° grid (12.5°–13.5°N and 81.5°–82.5°E) (https://www.nodc.noaa.gov/OC5/woa13/woa13data.html) proximal to the present sediment core location. The red colour filled circle is the water-depth at the core location.
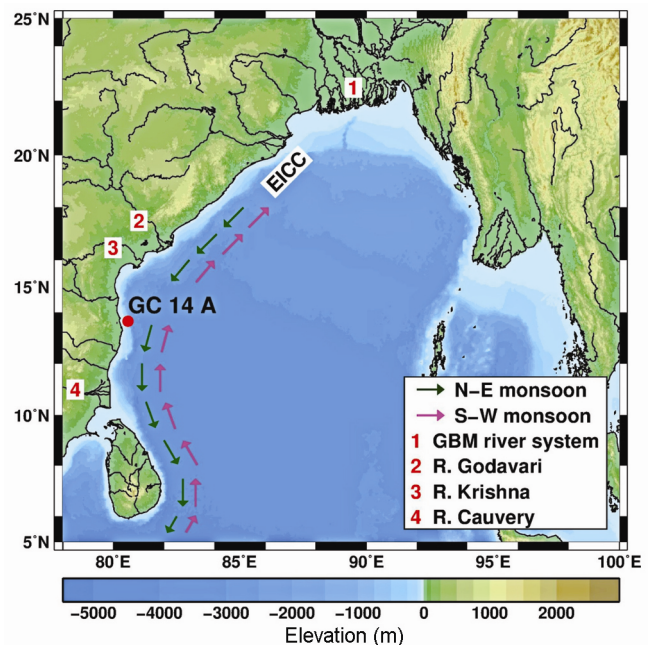


**Figure 2.** Location of GC-14A sediment core used in the present study (red filled circle). The seasonally reversing East India Coastal Currents (EICC), which disperse the sediment along the east coast of India are shown with coloured arrows (blue: during Northeast monsoon; pink: during Southwest monsoon).

expressed consecutive depleted – and enriched – $\delta^{18}O_{G.sacculifer}$ events identified as Bølling- llerød (BA: 14.7–12.7 ka) and Younger Dryas (YD: 12.7–11.7 ka) respectively, were used as tie-points to tune the ages of intermediate sections with the chronology of a nearby sediment core (SK218/A) having eight radiocarbon dates[13].

Sixty four salt-free, finely ground, oven-dried and accurately weighed sediment sub-sections were digested open in PTFE beakers using HF and $HClO_4$. The incipiently-dried digest was dissolved in 5 ml of supra-pure 0.5 M $HNO_3$ and diluted to 20 ml with deionized water for bulk sediment composition analysis (Supplementary Table 1). The Japanese Manganese Nodule Standard (JMS-1) and USGS Cody Shale (SCo-1) were used to monitor the accuracy of results. The analyses were done on Perkin-Elmer Optima 7300 DV ICP-OES calibrated with 5 matrix-matched multi-element calibration standards. The measured and reported values for the reference standards are given in Supplementary Table 2. The $C_{org}$ in the de-carbonated sections of the upper 2.08 m of the sediment core corresponding to a maximum age of 32 ka was measured on Thermo Flash Elemental Analyser (EA). The $C_{org}$ measurements are accurate to within ±1% as obtained for 2,5-bis(5-tert-butyl-2-benzoxazol-2-yl)thiophene (BBOT) standard. The $\delta^{13}C_{org}$ in few samples was measured on Thermo Delta-Plus IRMS coupled with EA.

Forty sediment sections were subjected to the extraction of dispersed sedimentary authigenic oxide particulate fraction following the standard procedure[14,15], which involves de-carbonation with 10% (v/v) acetic acid followed by leaching by 0.02 M hydroxylamine hydrochloride in 25% (v/v) acetic acid. The dried leachate dissolved in 0.05 M $HNO_3$ was analysed on Thermo ICP-MS calibrated with Japanese Mn-nodule reference material. The USGS A-1 and P-1 Mn-nodule reference standards were used to monitor the effectiveness of the leaching procedure. The analysed results for redox-sensitive Mn and Co in reference standards (MnO = 24.2% and Co = 0.34% as against certified values of 23.9% and 0.31% respectively, in USGS A-1, and 36.2% and 0.21% against certified values of 37.6% and 0.22% in USGS-P1) indicate complete leaching of oxides. The simple regression analysis of the compositional data was carried out using a statistical tool 'Correl' available with Microsoft Excel.

The radiocarbon age for the core-top section is 1.8 ka and for bottom section (282 cm) is 42.7 ka. The overall $\delta^{18}O_{G.sacculifer}$ variation is ~2.6‰ to 0.5‰ with distinct depletion at 14–15 ka and 10–1.8 ka and enrichment at 38–36, 31–26 and ~12 ka. The holocene/marine oxygen
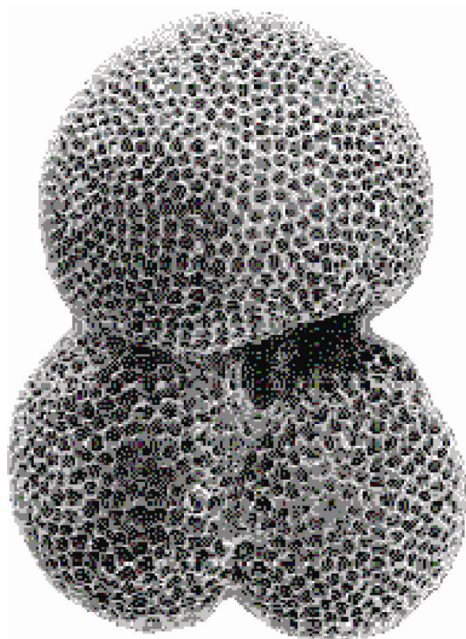


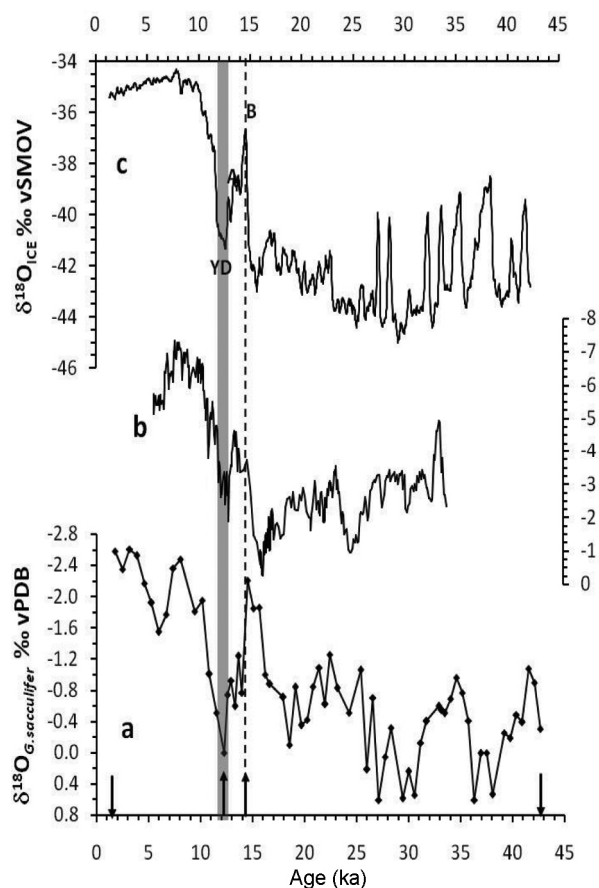**Figure 3.** Upper mixed layer dwelling planktonic foraminifera *Globigerinoides sacculifer* utilized for the oxygen isotope measurement. (Source: www.weiky.gl.ntu.edu.tw.)



**Figure 4.** (*a*) The time-series of $\delta^{18}O_{G.sacculifer}$ (Figure 3) is compared with (*b*) $\delta^{18}O$ of Mawmluh Cave deposit of Meghalaya[18] and (*c*) 10-point running mean of NGRIP ice-core $\delta^{18}O$ (ref. 17). Two measured radiocarbon ages are shown with downward arrows and two tie-points (Younger Dryas and Bølling) adopted from a nearby radiocarbon dated sediment core[13] are shown with upward arrows.

**Table 1.** Comparison of major element composition of bulk sediment of GC-14A sediment core with bulk sediment composition of sediment sources for the core-location (data from ref. 33)

|  | Present study average ($n = 64$) | Krishna River | Kaveri River | Godavari River | Average |
|---|---|---|---|---|---|
| Al (wt.%) | 6.1 | 3.4 | 4.8 | 4.3 | 4.2 |
| Fe (wt.%) | 4.8 | 4.2 | 1.8 | 5.7 | 3.9 |
| Ti (wt.%) | 0.4 | 0.6 | 0.3 | 0.9 | 0.6 |
| Mg (wt.%) | 1.4 | 1.3 | 1.1 | 1.4 | 1.3 |
| Mn (wt.%) | 0.02 | 0.10 | 0.03 | 0.10 | 0.07 |
| Ca (wt.%) | 9.0 | 5.3 | 1.1 | 4.5 | 3.6 |

isotope stage-2 (LGM) boundary is identified at 11 ka and the LGM conditions appear to have commenced at ~38 ka lasting until ~18 ka. This timing of LGM conditions is nearly consistent with the thoroughly evaluated timing of the evolution of LGM by Clark et al.[16]. The $\delta^{18}O_{G.sacculifer}$ time-series is punctuated by warm interstadials at 35–30 ka and at 25–20 ka suggesting that the oxygen-isotopic response of BoB surface to LGM climate is not smooth. Further, the BA and YD, typical of Greenland ice-cores[17] are clearly reflected in the deglacial section of the $\delta^{18}O_{G.sacculifer}$ time-series (Figure 4). Such D–O type of climate variability is also reported in cave deposits of Meghalaya[18] and other sedimentary records from the eastern margin of India[13] and from Arabian Sea[19–21], which formed the basis for reconstructing ISM variability. Hence, the present $\delta^{18}O_{G.sacculifer}$ time-series can be interpreted in terms of ISM intensity.

The ISM and northern high-latitude climate teleconnection is well-known, wherein the strengthening/ weakening of the ISM has been associated with the warm BA/cold YD[19,20]. The ISM intensity appears to have remained nearly constant during LGM as the overall variation of $\delta^{18}O_{G.sacculifer}$ is within ±0.5‰ around an average of −0.6‰ (Figure 4). However, there are two intervals of weakened ISM at ~28 and ~38 ka within the redefined LGM[16] reflected by enriched $\delta^{18}O_{G.sacculifer}$ up to 0.5‰. These events may be the combined signals of a set of cold-stadials in the D–O type climate oscillations as they approximately coincide with their timings in Greenland ice-core (Figure 4). The dramatic shifts in $\delta^{18}O_{G.sacculifer}$ from 0.2‰ down to −2.2‰ at the BA and from −2.2‰ up to 0.0‰ at the YD suggest extreme intensification followed by rapid weakening of the ISM. Thus, ISM appears to have been remarkably unstable during the deglacial transition[19–23]. A moderate enrichment of $\delta^{18}O_{G.sacculifer}$ is evident at 5–6 ka (Figure 4) suggesting mid-Holocene weakening of ISM. This weakened ISM (drought) is similar to that observed ~5 ka in other BoB sedimentary records[24], cave deposits[18] and Tibetan Lake sediments[25] that caused the beginning of growth of Harappan Civilization[26].

The modern ISM intensity influences the discharge of terrigenous clastics by peninsular rivers, which in turn might have influenced the status of BoB-OMZ[27]. However, whether ISM-OMZ coupling existed in the past-BoB is not known and can be understood with the help of geochemical tools.

The depositional site of the present sediment core is bound in the north by discharge points of Krishna-Godavari rivers and in the south by Kaveri River (henceforth together 'KGK') (Figure 2). These river basins share a common tectonic and sedimentation history[28] and the sediment discharged by them reaches the mid-slope region of the BoB[29]. Thus, the present core location represents a regional characteristic of sediments derived from KGK. Several marine transgressions have been recorded in the KGK basins since their opening in Cretaceous[30]. The upper 300 m thick sediment of the offshore KGK composed mainly of clay and silt deposited from Pleistocene to Recent[31]. In the light of this observation and progressive radiocarbon ages with depth in the present sediment core as well as in another nearby sediment core[13], it is unlikely that the sedimentation hiatus evident in Kaveri River basin during the marine isotope stage 5 to Holocene[32] had influenced offshore sedimentation. Except for the climate forced gradual sea level changes, there are no records of tectonic events in KGK basins during the time-period covered by the present sediment core. Therefore, the present record of terrigenous input variation may be considered as a reliable proxy for ISM variability.

The average composition of major elements (Al = 6.1%, Ti = 0.4%, Fe = 4.8% and Mg = 1.5%) (Supplementary Table 1) is nearly similar to the average composition of KGK sediment[33] (Table 1), as well as Kaveri sediment (Al = 6.6%, Ti = 0.3% and Fe = 2.9%)[34]. The minimum Ca content in the present core is 2.2% (Supplementary Table 1), which is also similar to the average Ca content of KGK (3.6%) (Table 1) and Kaveri sediment (Ca = 2.3%)[34]. Thus, the Ca content of 2.2% in the present core is accountable for terrigenous component and any higher Ca than this would indicate the presence of calcium carbonate. The microscopic observations of the coarse fractions indicate that the sediment sections with higher Ca correspond to the sections with abundant foraminifera. Hence, the calcium carbonate component is biogenic.

A mutually strong sympathetic association of Al, Ti and Mg ($r > 0.8$; $n = 64$) and their inverse association ($r > -0.5$) with Ca (Supplementary Table 3), as well as the co-variation of $C_{org}$ with Ca in their time-series (Figure 5) together support presence of terrigenous clastics and biogenic calcite phases in the sediment. The minor elements V, Cr and Zn are associated with the terrigenous phase as evident from their strong sympathetic association ($r > 0.7$) with terrigenous group elements and inverse association with biogenic Ca (Supplementary Table 3). A noteworthy depletion of Mn throughout the sediment core (Mn < 0.04%) (see Supplementary Table 1) compared to the average KGK sediment (Mn = 0.07%) (Table 1) suggests that the sediment core location (325 m water depth) has been under reducing condition since the last 42 kyr, because, under the influence of OMZ, the sedimentary-Mn is reduced and redirected to overlying OMZ-water[35]. Considering that the average terrigenous sediment supplied to the core-location had around 0.07% of Mn, the 0.02% to 0.04% of Mn recorded in the bulk sediment (Supplementary Table 1) must be a result of its partial loss from the sediment under extreme reducing environment. Hence, its changes through time can provide qualitative information on the past variation of OMZ intensity[36].

The concentrations of Mn and Co in leachable fraction of the sediment core vary in a narrow range of 20–35 and 1–3 ppm respectively, and exhibit strong positive association with each other ($r = 0.8$). Their mutual coherence is expected as both are remobilized in the sediment with decreasing oxygen below the sub-oxic level. A significantly low leachable Mn and Co, than in the bulk composition of the sediment core (average Mn = 250 ppm and

Co = 8.7 ppm) (Supplementary Table 1) further confirm that the core location has always remained within the oxygen depleted environment throughout the last 42 kyr.

The minimum Ca content of 2.2% at 270 cm depth in core (Supplementary Table 1), that is considered as terrigenous-Ca, was subtracted from the bulk sediment Ca contents to obtain the biogenic-Ca. To extract the changes in input of terrigenous clastics, the bulk-composition is normalized by estimated biogenic-Ca in respective sub-sections. The inter-elemental associations obtained for the biogenic-Ca normalized bulk elements (Supplementary Table 4) exhibit stronger and clearer grouping of terrigenous elements ($r > 0.8$) than in the bulk composition ($r > 0.6$) (Supplementary Table 3) and confirm that all the major and minor elements except Ca are associated only with the terrigenous clastic phase.

The time-series of the identified two groups of elements provide information on changes in terrigenous
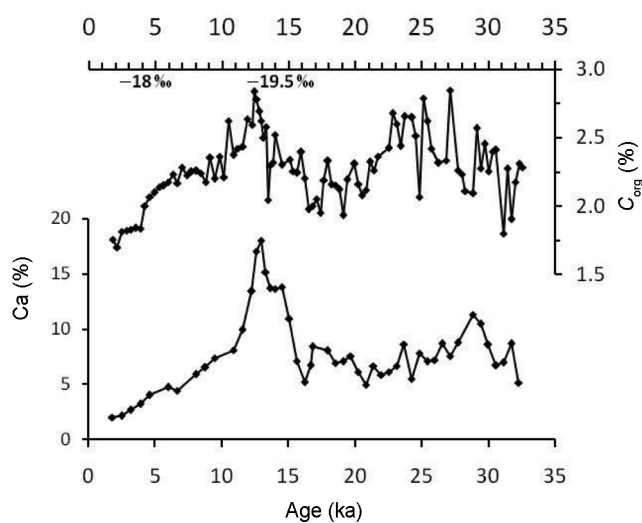


**Figure 5.** Productivity variation during the last 32 kyr recorded by organic carbon and biogenic carbonate-Ca in the studies sediment core. The values in the upper panel are the average of $\delta^{13}C_{org}$ in few samples belonging to ~16–12 ka and ~5–1.7 ka.
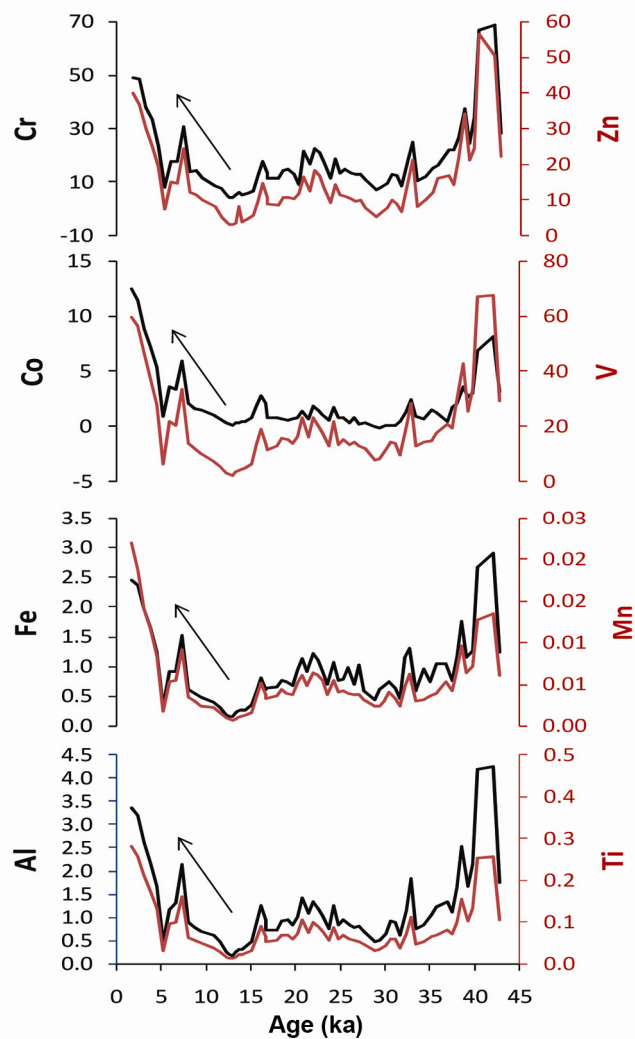


**Figure 6.** Time-series of carbonate-Ca normalized elemental composition. The colours of the lines are as those used for labels on the vertical axes of respective element panels.

input and productivity. The terrigenous elements exhibit distinct depletion between 35 and 15 ka bound by strongly enriched peaks during pre-LGM and the Holocene (Figure 6), suggesting that the KGK discharge was significantly lower during LGM and began to increase with the commencement of Holocene. This pattern of river discharge is not only consistent with our interpretation of LGM weakening and Holocene strengthening of the ISM based on $\delta^{18}O_{G.sacculifer}$, but also with several past monsoon records derived from sediments of the northern Indian Ocean[19,20,23,37]. The rapid weakening of ISM precipitation causing severe drought conditions within the Holocene at 5–4 ka (refs 24, 26) is also well-reflected by decreased contents of terrigenous elements (Figure 6) suggesting weakened river discharge.

The enhanced terrigenous matter input is expected to enrich coastal waters with nutrients and hence increase productivity[9]. To test this we assessed the $C_{org}$ and biogenic-Ca variation in the last 32 kyr. The $C_{org}$ shows distinct increase during deglacial period (16–12 ka) from ~2% to 2.7% and a monotonous decrease from ~2.7% to ~1.7% through the Holocene, with comparable trend in biogenic-Ca variation (Figure 5), which is in contrast to the terrigenous input (Figure 6). At the outset, the coherent increase (decrease) of $C_{org}$ and biogenic-Ca during deglacial transition (Holocene) suggest increased (decreased) marine production. The $\delta^{13}C_{org}$ of ~−19.5‰ (vPDB) during the deglacial transition is followed by an increase of ~2‰ through the Holocene indicating dilution of marine organic matter by soil-carbon, which justifies the observed contrasting trends of productivity and terrigenous input. The decreased productivity during Holocene is not expected in the light of intensification of BoB-OMZ due to enhanced productivity resulting from increased terrigenous loading in coastal waters during intensified ISM years[9]. We speculate that the increased terrigenous input due to increased turbidite discharge particularly in coastal waters reduce photosynthesis by light limitation and strengthened the freshwater plug preventing upwelling.

The sediment core retrieved from the core of modern OMZ off Chennai coast contains valuable information on summer monsoon intensity – terrigenous clastic input – OMZ linkage in the past.

The major and minor element composition of the sediments closely resembles the composition of source basin sediments indicating that seasonal rivers are mostly responsible for terrigenous clastic supply to the east-coast of India. The terrigenous sediment input has shown remarkable increase through the Holocene but with a distinct decrease at ~5 ka suggesting enhanced discharge of rivers throughout the Holocene except for sudden weakening during the mid-Holocene. The marine productivity appears to have decreased through the Holocene probably due to turbidite charging of the photic water due to intensified peninsular rivers.

The extreme depletion of redox-sensitive elements in the sediment as compared to their concentration in source basins suggests perennially intense OMZ-core in the region for the last 42 kyr.

1. Selvaraj, K. *et al.*, Evaluation of metal contamination in coastal sediments of the Bay of Bengal: geochemical and statistical approaches. *Mar. Pollut. Bull.*, 2004, **49**, 174–185.
2. Kolla, V. and Rao, N. M., Sedimentary sources in the surface and near surface sediments of the Bay of Bengal. *Geo-Mar. Lett.*, 1990, **10**, 129–136.
3. Goodbred Jr, S. L., Response of the Ganges dispersal system to climate change: a source-to-sink view since the last interstadial. *Sedimdent Geol.*, 2003, **162**, 83–104.
4. Tripathy, G. R. *et al.*, Major and trace element geochemistry of Bay of Bengal sediments: Implications to provinance and their controlling factors. *Paleogeogr., Palaeoclimatol., Palaeoecol.*, 2014, **397**, 20–30.
5. Bristow, L. A. *et al.*, $N_2$ production rates limited by nitrate availability in the Bay of Bengal oxygen minimum zone. *Nature Geosci.*, 2016; doi:10.1033/NGEO2847.
6. Jain, V. *et al.*, Evidence for existence of Persian Gulf Water and Red Sea Water in the Bay of Bengal. *Clim. Dynam.*, 2016; doi:10.1007/s00382-016-3259-4.
7. Long, M. C. *et al.*, Finding forced trends in oceanic oxygen. *Global Biogeochem. Cycles*, 2016; doi:10.1002/2015-GB005310.
8. Wyrtki, K., Oceanographic Atlas of the International Indian Ocean Expedition. National Science Foundation, Washington, DC, 1971, p. 531.
9. Sarma, V. V. S. S. *et al.*, Intenisified oxygen minimum zone in the western Bay of Bengal during summer monsoon: influence of river discharge. *J. Oceanogr.*, 2013, **69**, 45–55; doi:10.1007/s10872-012-0156-2.
10. Sengupta, S. *et al.*, Vertical variation of oxygen isotope in bay of Bengal and its relationships with water masses. *J. Geophys. Res. Oceans*, 2013, **118**, 6411–6424.
11. Dutta, K. *et al.*, IR correction values for the Northern Indian Ocean. *Radiocarbon*, 2001, **43**, 483–488.
12. Danzeglocke, U. *et al.*, 2008, CalPal-2007 online; http://www.calpalonline.de/ (accessed on 10 May 2008).
13. Govil, P. and Divakar Naidu, P., Variations of Indian monsoon precipitation during the last 32 kyr reflected in the surface hydrography of the Western Bay of Bengal. *Quat. Sci. Rev.*, 2011, **30**, 3871–3879.
14. Chester, R. and Hughes, M. J., A chemical technique for the separation of ferromanganese minerals, carbonate minerals and adsorbed trace elements from pelagic sediments. *Chem. Geol.*, 1967, **2**, 249–262.
15. Wilson, D. J. *et al.*, Reactivity of neodymium carriers in deep sea sediments: implications for boundary exchange and paleoceanography. *Geochim. Cosmochim. Acta*, 2013, **109**, 197–221.
16. Clark, P. *et al.*, The last glacial maximum. *Science*, 2009, **325**, 710–714.
17. North Greenland Ice Core Project members. High-resolution record of Northern Hemisphere climate extending into the last interglacial period. *Nature*, 2004, **431**, 147–151.
18. Dutt, S. *et al.*, Abrupt changes in Indian summer monsoon strength during 33,800 to 5500 years BP. *Geophys. Res. Lett.*, 2015, **42**, 5526–5532.
19. Schulz, H. *et al.*, Arabian Sea and Greenland climate oscillations of the past 110,000 years. *Nature*, 1998, **393**, 54–57.
20. Kessarkar, P. M. *et al.*, Variation in the Indian summer monsoon intensity during the Bølling-´llerød and Holocene. *Palaeoceanography*, 2013, **28**, 413–425.

21. Banakar, V. K. *et al.*, Indian summer monsoon forcing on the deglacial polar cold reversals. *J. Earth Syst. Sci.*, 2017; doi:10.1007/s12040-017-0864-5.

22. Sinha, A. *et al.*, Variability of Southwest Indian summer monsoon precipitation during the Bølling-´llerød. *Geology*, 2005, **33**, 813–816.

23. Deplazes, G. *et al.*, Links between tropical rainfall and North Atlantic climate during the last glacial period. *Nat. Geosci.*, 2013, **6**, 1–5.

24. Ponton, C. *et al.*, Holocene aridification of India. *Geophys. Res. Lett.*, 2012, **39**, 1–6.

25. Nishimura, M. *et al.*, Paleoclimatic changes on the southern Tibetan Plateau over the past 19,000 years recorded in Lake Pumoyum Co and their implications for the southwest monsoon evolution. *Palaeogeogr., Palaeoclimatol., Palaeoecol.*, 2014, **396**, 75–92.

26. Staubwasser, M. *et al.*, Climate change at the 4.2 ka BP termination of the Indus Valley Civilization and Holocene South Asian monsoon variability. *Geophys. Res. Lett.*, 2003, **30**; doi:10.1029/2002GL016822.

27. Dileep Kumar, M., *Biogeochemistry of the North Indian Ocean*, Indian Academy of Sciences, Bangalore, 2006.

28. Sastri, V. V. *et al.*, Stratigraphy and tectonics of sedimentary basin on East coast of peninsular India. *AAPG Bull.*, 1973, **57**, 655–678.

29. Purnachandrarao, V. and Kessarkar, P. M., Geomorphology and geology of the Bay of Bengal and the Andaman Sea. In *The Indian Ocean: A Perspective* (eds Sengupta, R. and Desa, E.), Balakema Publ., 2001, vol. 2, pp. 818–868.

30. Ramkumar, M. *et al.*, Deltaic sedimentation during Cretaceous period in northern Cauveri basin, South India: facies architecture, depositional history and sequence stratigraphy. *J. Geol. Soc. India*, 2004, **66**, 81–94.

31. Anitha, G. *et al.*, Shallow geological environment of Krishna-Godavari offshore, Eastern Continental margin of India as inferred from the interpretation of sparker data. *J. Earth Syst. Sci.*, 2014, **123**, 229–342.

32. Alappat, L. *et al.*, Chronology of Cauvery delta sediment from shallow subsurface cores using elevated temperature post-IR IRSL dating of feldspar. *Geochronometria*, 2010, **37**, 37–47.

33. Subramanian, V. *et al.*, Chemical composition of river sediments from the Indian subcontinent. *Chem. Geol.*, 1985, **48**, 271–279.

34. Dekov, M. *et al.*, Chemical composition of sediment and suspended matter from the Cauveri and Brhamaputra rivers (India). *Sci. Total Environ.*, 1998, **212**, 89–105.

35. Dickens, G. R. and Owen, R. M., Late Miocene–Early Pliocene manganese redirection in the central Indian Ocean: expansion of the intermediate water oxygen minimum zone. *Palaeoceanography*, 1994, **9**, 169–180.

36. Schenau, S. J. *et al.*, Oxygen minimum zone controlled Mn redistribution in Arabian Sea sediments during the late Quaternary. *Palaeoceanography*, 2002, **17**; doi:10.1029/2000PA000621.

37. Miriyala, P. *et al.*, Increased chemical weathering during the deglacial to mid-Holocene summer monsoon intensification. *Sci. Rep.*, 2017; doi:10.1038/srep44310.

# Multiple regression analysis of geoelectric imaging and geotechnical site investigation test results

**Rambhatla G. Sastry[1,*], Sumedha Chahar[1] and Mahendra Singh[2]**

[1]Department of Earth Sciences, and
[2]Department of Civil Engineering, IIT Roorkee, Roorkee 247 667, India

**Geotechnical site characterization through non-invasive and cost-effective electrical resistivity imaging (ERI) and induced polarization imaging (IPI) offers promise compared to conventional point-geotechnical site investigations (standard penetration test, SPT), for which a basic understanding of factors (grain size (sand, fines) and water content) influencing them is needed. Here we perform a multiple regression analysis of ERI, IPI and SPT results in a site investigation at Lucknow, India. The results show that grain size and water content influence both chargeability and SPT values in a similar manner, while resistivity values are affected differently with a low RMS prediction error for chargeability.**

GEOMECHANICAL properties of near surface soils are routinely estimated through analysis of soil samples and invasive geotechnical testing that could include, for example, the standard penetration test (SPT), static cone penetration test (SCPT) and dynamic cone penetration test (DCPT)[1,2]. Although these geotechnical tests provide high-resolution data to geotechnical engineers, their acquisition is fraught with heavy budgets as well as invasive and time-consuming methodologies. Furthermore, SPT and SCPT are not feasible for hard strata at shallow depths[1,2], but knowledge of geomechanical properties to sufficient depths is needed for major civil constructions. The possibility of predicting site geotechnical test results through a conjunctive use of geoelectrical (electrical resistivity imaging (ERI) and induced polarization imaging (IPI)) and few geotechnical data was explored[3]. Electrical data and SCPT results to delineate the subsurface lithological units were used[4]. It is well known among the geotechnical community that the SPT-N value is directly proportional to grain size and clay content, and inversely proportional to porosity and water content[1,2,5]. However, the relationship between geotechnical parameters and geophysical measurements has been studied by only a few researchers. Resistivity of earth materials is inversely proportional to porosity, clay content and water content whereas

*For correspondence. (e-mail: rgss1fes@iitr.ac.in)